A Hybrid Coupled-Resonator Bandpass Filter Topology Implemented on Lossy Semiconductor Substrates

Robert C Frye, Kai Liu*, Guruprasad Badakere** and Yaojian Lin**

RF Design Consulting, LLC, Berkeley Heights, NJ, 08854, USA, *STATS ChipPAC, Inc, Tempe AZ, 85284, USA, **STATS ChipPAC, Ltd Singapore 768442

***Abstract* — The Q of filter resonators formed on lossy substrates depends on their mode of excitation. Modifying the circuit design such that the voltage signals on resonator coils is predominantly differential can result in substantially higher Q. Band-pass filter resonator topologies that exploit this difference are discussed, and experimental results are presented for 802.11b band-pass filters implemented in a thin-film technology on silicon substrates.**

***Index Terms* — Bandpass filters, circuit topology, passive circuits, thin-film inductors.**

I. Introduction

It has been observed in RF ICs that the effective Q of on-chip inductors is higher in differential than in single-ended operation [1]. In single-ended operation, the average potential of the inductor coil varies with respect to the grounded substrate. The dissipation resulting from displacement currents flowing in and out of the lossy substrate lowers the overall Q of the device. In differential-mode operation, however, the average potential of the inductor coils with respect to ground is a constant. The fluctuating electric fields in the inductor are confined to inter-winding fields. These may penetrate into the lossy substrate, giving rise to some capacitive loss, but overall the effect is much less than in single-ended operation. (Inductive losses arising from eddy currents in the lossy substrate are the same in both cases.)

The band-pass filters described in this paper are built using a thin-film integrated passive device (IPD) technology on silicon substrates. A cross-section of the structure is shown in Fig. 1. It consists of two layers of metal (M2 and M3) with polyimide interlevel dielectric. A third metal layer (M1) is used exclusively for the bottom electrode of the capacitors.

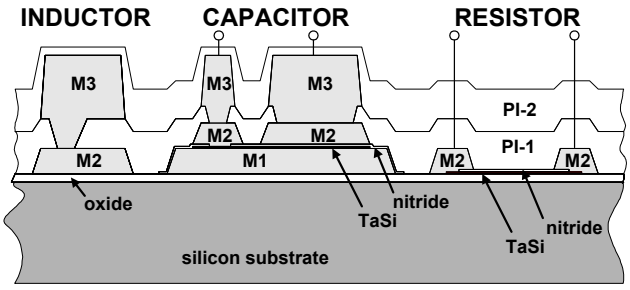

Fig. 1. Thin-film integrated passive device (IPD) structure.

The two bottom layers of metal are aluminum, and the top layer, used for the inductor coils, is an 8μm thick layer of copper. The substrates are specially treated to have substantially lower loss than the silicon used in conventional silicon RF ICs, but still have some impact on inductor Q at high frequency.

Equivalent circuit models of monolithic spiral inductors on semiconductor substrates have been well-studied, especially with the more recent advent of silicon RF ICs [2]. The maximum obtainable Q in RF integrated circuit technology is limited by a number of factors, including the typically thin metal layers, restricted available area (because of cost) and the lossy silicon substrates, which are usually on the order of 20 Ω·cm. The structure shown in Fig. 1 circumvents these problems by the use of a thick top copper layer and substantially reduced substrate loss. However, although the Q is significantly higher in IPD technology, it is still degraded to some extent by substrate losses.

Fig. 2 compares simulated [3] effective inductance and Q for a typical example IPD inductor. At lower frequencies, there is little difference between the two cases. In this example, the difference in Q becomes apparent above 1.5GHz, and is quite pronounced above 2.5GHz. Note, also, that the self-resonant frequency in differential-mode operation is substantially higher. In the results shown in Fig. 2, the component is characterized in a one-port configuration. The effective induc-

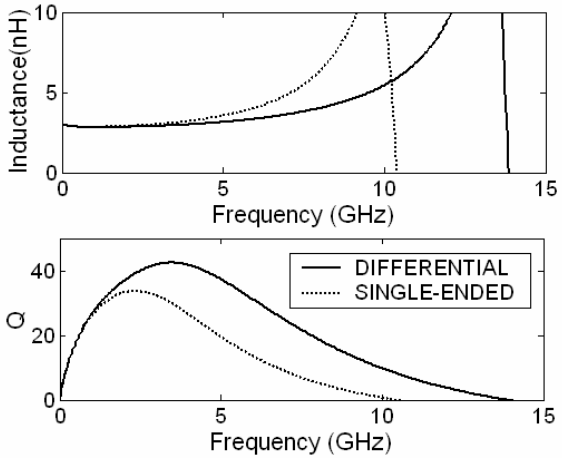

Fig. 2. Comparison of simulated inductance and Q for a typical example IPD inductor in differential and single-ended operation.

tance and Q are determined in the conventional way from the impedance,

$$L = imag(Z)/(2\pi f) \tag{1}$$

and

$$Q = imag(Z)/real(Z). \tag{2}$$

II. Resonator Design

Fig. 3 shows three alternative resonator circuits. Resonator A is a simple parallel LC resonator, with a resonant frequency given by

$$f_{RES} = 1/(2\pi\sqrt{LC}). \tag{3}$$

For resonator A, the inductor is operated in a single-ended mode. At resonance, the impedance of the resonator is real, so Eq. 2 is not valid for calculation of the resonator Q. Instead, resonator Q can be determined from the phase of the impedance, ϕ. It is given by

$$Q = -\frac{f}{2}\frac{d\phi}{df}. \tag{4}$$

Resonator B in Fig. 3 has the same resonant frequency as A. The addition of the capacitor in series with the inductor gives rise to an impedance zero below the resonant frequency. At resonance, however, the inductor in this circuit operates in differential mode- i.e. the voltage amplitudes on its terminals are equal, and they are 180º out of phase.

Table I lists comparisons of the Q of the various resonator circuits shown in Fig. 3. For these comparisons, the capacitor values were adjusted to obtain resonance at 2450MHz. For a simple model of the inductor, consisting of a series RL circuit, the Q of the resonator calculated from Eq. 2 is identical to the inductor Q (assuming lossless capacitors) for all three resonators. (The series resistance in this case was chosen to give an inductor Q of 30 at 2450MHz.) However, using the more accurate simulation model of the inductor (the example shown in Fig. 2) the Q of resonator B is higher. It can be readily verified that this difference arises from the differential mode of operation by comparing the performance of resonator B with that of resonator C. For inductors without shunt losses, these two circuits show identical performance. However, because the inductor in resonator C operates in single-ended mode, for inductors with appreciable shunt losses resonator C has lower Q than resonator B.

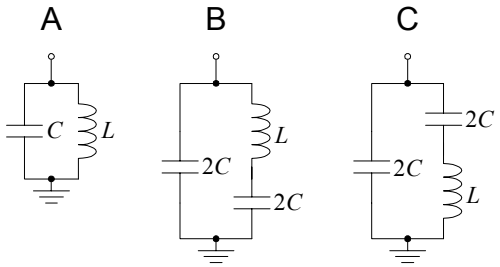

Fig. 3. Resonator circuits.

TABLE I
Resonator Q Comparison

resonator	Q @ 2450MHz	
	RL model	EM sim model
A	30	35.2
B	30	40.5
C	30	35.2

III. Band Pass Filter Topologies

Most band-pass filter topologies used in thin-film technology are of the coupled-resonator type. The advantage of coupled-resonator filters is that they do not require a wide range of inductance values, and are often realized using the same inductance for all resonators. Fig. 4 shows some alternative band-pass filter topologies. For the top-coupled and shunt-coupled topologies, filter synthesis techniques can be used to derive circuits that approximate desired response characteristics near the pass band (e.g. Chebyshev, Bessel, etc) but the attenuation characteristics of these filters differ significantly outside the pass band.

The top-coupled topology is one of the most commonly used. It is especially suitable for 802.11b/g receive filters because it offers high attenuation below the pass band. This helps to attenuate strong blocking signals in the cellular communications bands. Note, however, that in this circuit the resonators operate in a single-ended mode.

An advantage of the shunt-couple topology is that by properly distributing series capacitors on either side of the inductors, the inductors can be made to operate in predominantly differential mode around the pass band. The resulting higher resonator Q leads to lower pass band insertion losses. A disadvantage, however, is that the shunt-coupled topology has poor attenuation below the pass band.

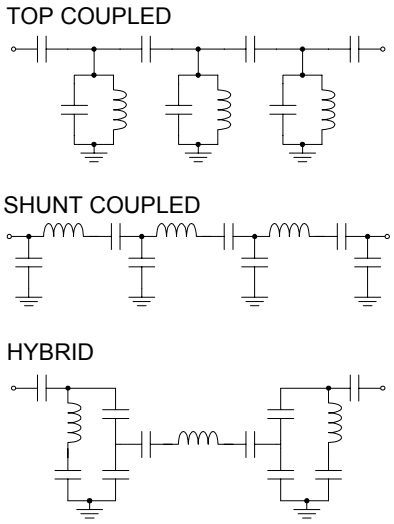

Fig. 4. Several alternative 3rd-order band-pass filter topologies.

The hybrid topology shown in Fig. 4 incorporates some of the best elements of both. In this circuit, the two outer resonators are top coupled, and the inner one is shunt coupled. The outer top-coupled resonators have added series capacitors, as in resonator B in Fig. 4, resulting in improved resonator Q. This resonator structure also results in added attenuation poles below the pass band, which enhances the low-freqency attenuation of the filter. Resonators of this type have been previously described for this purpose [4].

IV. Experimental Comparison

Three filters, corresponding to the three topological variations in Fig. 4, were designed and fabricated in the thin-film IPD technology described above. Fig. 5 shows micrographs of these three filters. Each filter measured roughly 1.7 X 1.5 X 0.25 mm. The inductor coils used in each of the filters, as well as their general arrangement, was nearly identical. For convenience in evaluation, these filters were designed to be evaluated by RF wafer probe. The filters were designed for 802.11b operation, with a passband from 2400 to 2500MHz. With the fixed coil arrangement, detailed design of the filters used an iterative method of circuit and electromagnetic simulation to determine the capacitor values [5].

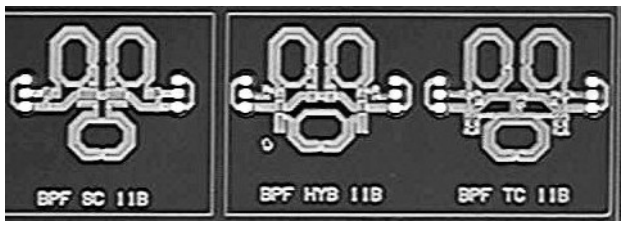

Fig. 5 Micrograph of three bandpass filters using different coupled-resonator topology, implemented in thin-film IPD technology on silicon substrates.

Measured characteristics of the three designs are shown in Fig. 6. As mentioned above, the top-coupled topology is especially well-suited for 802.11b/g because of the high attenuation in the cellular bands from 800 to 1900MHz. However, the top-coupled topology has relatively poor attenuation above the pass band. By contrast, the shunt-coupled topology has very good attenuation above the pass band, and relatively poor attenuation below. The hybrid topology incorporates some of the best features of both.

The attenuation characteristics of the three filters are summarized in Table II. Direct comparison of the insertion loss is complicated by the fact that the designed bandwidth of the top-coupled filter was narrower than that of the other two. This was done to obtain a modest degree of attenuation in the 802.11a band at 5 to 6 GHz. This difference exaggerates the difference in insertion loss, which is about 0.8dB in the measured devices. It can be estimated from simple power loss considerations that the improvement attributable to the difference in resonator Q arising from differential versus single-ended operation is about 0.2dB in these examples. The remainder of the difference arises from circuit design. Combined with the other performance advantages, the difference between the hybrid and top-coupled topologies in insertion loss for comparable stop-band attenuation is considerable.

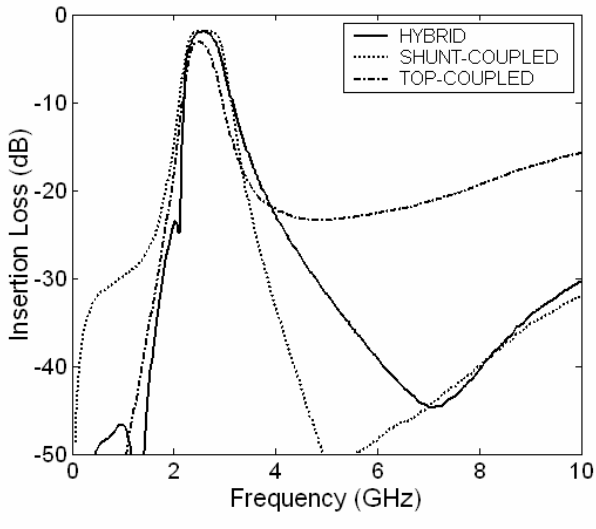

Fig. 6. Measured characteristics of the wafer-probe filters.

TABLE II
Filter Attenuation Comparison

Band	freq. (MHz)	attenuation (dB)		
		Top coupled	Shunt coupled	Hybrid
GSM	824-960	57-52	31-30	49-51
DCS	1710-1990	29-21	22-16	32-25
802.11b/g	2400-2499	2.4-2.5	1.7-1.6	1.8-1.6
802.11a	5115-5825	23-22	53-46	34-42

V. Practical Implementation

The wafer-probe filters demonstrate the differences in the various filter topologies. However, features of the wafer-probe designs make them unsuitable for practical use. In system-in-package (SiP) assemblies, IPD filters are typically diced into small, chip-like components and are connected using either wire-bond or flip-chip technology into a package alongside an active die. In the wafer-probe designs, the ground return path is integral to the circuit design, and has a significant impact on the characteristics. In practical assemblies, the package provides most of the ground return path. Consequently, the circuit design requires some minor modification. A practical design can use the same topology and general arrangement, but requires some adjustment in component values.

Fig. 7 shows a micrograph of a flip-chip filter using the hybrid topology. This design is smaller than the wafer-probe

example, measuring 1.35 X 1.1mm. The component is shown

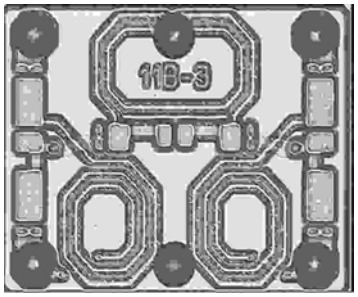

Fig. 7. Micrograph of a 3rd-order flip-chip 802.11b band pass filter using the hybrid circuit topology.

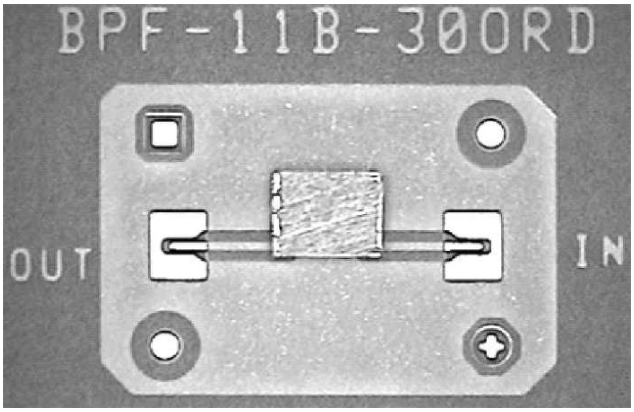

Fig. 8. Test board configuration, showing the IPD mounted face-down using flip-chip attachment.

assembled on a test board in Fig. 8. This circuit also has an added capacitor in parallel with the shunt-coupled inductor coil. This capacitor adds an attenuation pole above the pass band, resulting in characteristics that are similar to those of elliptic bandpass filters.

The test board consisted of a pair of coplanar transmission lines connecting to the input and output of the filter, which is flip-chip mounted face-down on the board. The surrounding ground plane also connects to the filter, and provides the ground return path for the filter. Connection to the board was made by RF probes at the ends of the transmission lines. The use of probes eliminates the need to de-embed connector characteristics, which usually interferes with accurate determination of the insertion loss in the pass band. The simulated and measured characteristics are shown in Fig. 9. Measured insertion loss over the passband of this filter was 1.4 to 1.5 dB.

VII. Conclusion

Modifying the circuit topologies of the resonators in bandpass filters so that the signal voltage at resonance is differential improves the resonator Q for lossy substrates. For the particular technology used in this study, the improvement in resonator Q is typically 12 to 15%. The topological modifications to the circuit alter the shape of the overall attenuation characteristics, making it impossible to directly compare losses with and without the modified resonator topology, but from simple energy loss estimates, it can be determined that this modification improves the passband insertion loss by about 0.2dB. In other technologies, especially those fabricated on semiconductor substrates with lower resistivities and higher losses, the improvement may be even more significant.

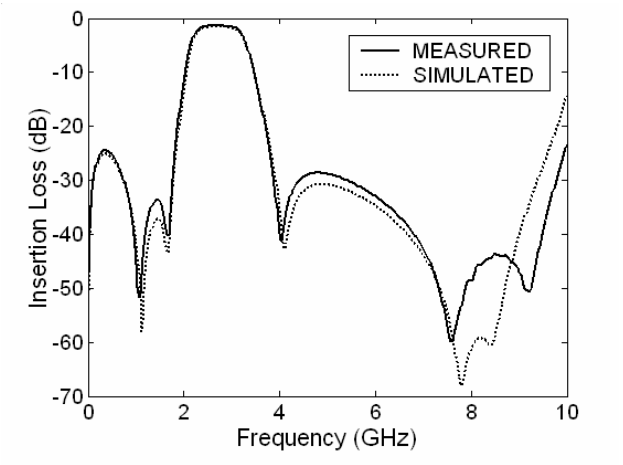

Fig. 9. Measured and simulated characteristics of the flip-chip 802.11b band-pass filter.

In addition to mitigating the effects of substrate losses, the hybrid filter topology incorporates some of the desirable features of both top-coupled and shunt-coupled bandpass filters. The modified top-coupled resonator provides added attenuation below the passband, and the incorporation of a shunt-coupled stage improves attenuation above the passband. Because all of the inductors in this topology operate in a predominantly differential mode, the effects of capacitive coupling to lossy substrates are minimized.

REFERENCES

[1] M. Danesh and J. R. Long, "Differentially Driven Symmetric Microstrip Inductors," IEEE Trans. Microwave Theory and Techniques, 50, 1, 332-341, January 2002.

[2] J. R. Long and M. A. Copeland, "The Modeling, Characterization and Design of Monolithic Inductors for Silicon RF IC's," IEEE J. Solid-State Circuits, 32, 3, 357-369, March 1997.

[3] S. Kapur and D. Long, "Large-Scale Full-Wave Simulation," Proc. 41st Design Automation Conference, 806-809, San Diego, CA, June 7-11, 2004.

[4] J.-S. Lim and D. C. Park, "A Modified Chebyshev Bandpass Filter with Attenuation Poles in the Stopband," IEEE Trans. Microwave Theory and Techniques, 50, 1, 332-341, January 2002.

[5] K. Liu aand R. C. Frye, "Full-Circuit Design Optimization of a RF Silicon Integrated Passive Device," Proc 15th IEEE Topical Meeting on Electrical Performance of Electronic Packaging, 327-330, Scottsdale, AZ, Oct. 23-25, 2006.